Int. J. Electrochem. Sci., 6 **(2011)** 5689 - 5700

International Journal of
ELECTROCHEMICAL
SCIENCE
www.electrochemsci.org

Cefacetrile as Corrosion Inhibitor for Mild Steel in Acidic Media

Ashish Kumar Singh[*], *Sudhish Kumar Shukla, Eno E. Ebenso*

Department of Chemistry, School of Mathematical and Physical Sciences, North-West University (Mafikeng Campus), Private Bag X2046, Mmabatho 2735, South Africa.
[*]E-mail: singhapc@gmail.com

Received: 13 September 2011 / *Accepted:* 19 October 2011 / *Published:* 1 November 2011

The corrosion inhibition of mild steel in acidic media using Cefacetrile was investigated by using various corrosion monitoring techniques such as weight loss, potentiodynamic polarization and electrochemical impedance spectroscopy. All the techniques used for the studies showed the increase in inhibition efficiency and decrease in the corrosion rate by increasing the inhibitor concentration. Langmuir adsorption isotherm and impedance studies showed that CFT inhibits through adsorption mechanism. Potentiodynamic polarization reveals that CFT acted as mixed-type predominantly cathodic inhibitor. The mechanism of corrosion inhibition is also proposed.

Keywords: Cefacetrile: Mild steel; Acid inhibition; EIS; kinetic; Thermodynamic parameters

1. INTRODUCTION

Mild steel is widely applied as the constructional material in many industries due to its excellent mechanical properties and low cost. The main problem of applying mild steel is its dissolution in acidic solutions. Recently, the inhibition of mild steel corrosion in acid solutions by different types of organic inhibitors has been extensively studied [1-8].

Corrosion inhibitors are used in eliminating the undesirable destructive effect and in preventing the metal dissolution. Most of the available inhibitors are toxic compounds that should be replaced by new inhibitors in the environmental protection. The research for effective and acceptable corrosion inhibitors instead of the toxic inhibitors becomes necessary in inhibition of mild steel corrosion in acid solutions [9, 10]. The efficiency of an organic compound as a successful inhibitor is mainly dependent on its ability to get adsorbed on the metal surface. Aliphatic amines [11] such as dimethylamine, ethylamine, diethylamine, butylamine, butyldiethylamine and other derivatives of octylamine inhibit the corrosion of steel in acid solution by donating the unshared pair of electrons from the N atom and

form a surface complex. However, only a few non-toxic and eco-friendly compounds have been investigated as corrosion inhibitors. Ceftriaxone [12], Tryptamine [13], Succinic acid [14], L-ascorbic acid [15], sulfamethoxazole [16], cefazolin [17], disulfiram [18] and cefatrexyl [19] were found to be effective inhibitors for acid environments. The inhibitive effect of four antibacterial drugs, namely ampicillin, cloxacillin, flucloxacillin and amoxicillin towards the corrosion of aluminium has been investigated [20]. The inhibition action of these drugs was attributed to blocking the surface via formation of insoluble complexes on the metal surface.

The objective of this study is to investigate the corrosion behaviour of mild steel in 1M HCl solution at 308 K in the presence of Cefacetrile (CFT) using weight loss, polarization resistance, Tafel polarization and electrochemical impedance techniques. The effects of temperature, acid concentration, immersion time were also studied. Several isotherms were tested for their relevance to describe the adsorption behaviour of the studied compound.

2. EXPERIMENTAL PROCEDURE

2.1 Material preparation

The mild steel coupons having composition (wt %): C = 0.17, Mn = 0.46, Si = 0.26, S = 0.017, P = 0.019 and balance Fe were used for weight loss measurement and of size 1.0 cm × 1.0 cm (exposed) with a 7.5 cm long stem (isolated with commercially available lacquer) were used for electrochemical measurements. The mild steel samples were polished with emery paper of 600 - 1200 grades, washed thoroughly with doubled distilled water, degreased with acetone and finally dried. 1M HCl solution was used in all studies (except in acid concentration studies). Its chemical structure of Cefacetrile (CFT) is shown in figure 1. The inhibitor concentration in the weight loss and electrochemical study was in the range of 20 to 100 ppm by weight.

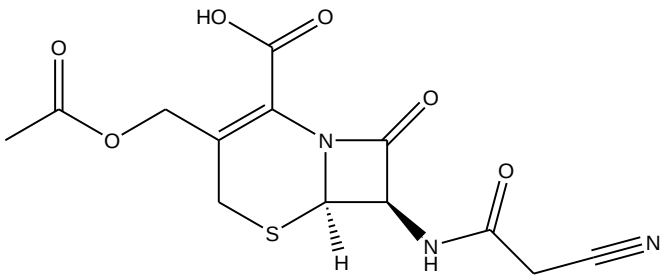

Figure 1. Molecular structure of Cefacetrile (CFT) molecule

2.2 Weight loss studies

Weight loss experiments were done according to the method described previously [21]. The mild steel coupons of 2.5 cm x 2.0 cm x 0.025 cm were abraded with a series of emery paper (grade

600-1200). After weighing accurately, the specimens were immersed in 100 ml conical flask containing 100 ml 1 M HCl solution with and without different concentration of inhibitor. All the solutions were covered. After 3 h (except in immersion time studies), the specimens were taken out, washed, dried and weighed accurately. All the experiments were performed in triplicate and average value reported. The inhibition efficiency (η %) and surface coverage were determined by using the following equations [22] :

$$\eta\ \% = \frac{w_o - w_i}{w_o} \times 100 \quad (1)$$

$$\theta = \frac{w_o - w_i}{w_o} \quad (2)$$

where, w_o and w_i are the weight loss value in absence and presence of inhibitor, respectively.

2.3 Electrochemical measurements

The electrochemical experiments were carried out using Gamry Potentiostat / Galvanostat (model 600) with EIS software, Gamry-Instruments Inc., USA, in a conventional electrolytic cell with three electrode arrangements: saturated calomel reference electrode (SCE), platinum foil of 1 cm x 1 cm as a counter electrode and mild steel coupons of size 1.0 cm × 1.0 cm (exposed) with a 7.5 cm long stem (isolated with commercially available lacquer) as working electrode. Prior to each experiment, the mild steel specimen was treated similarly as in weight loss experiments. The electrode potential was allowed to stabilize 30 min. before starting the experiments. All experiments were conducted at room temperature.

The Tafel polarization curves were obtained by changing the electrode potential automatically from (+ 500 mV to – 500 mV) at open circuit potential with a scan rate 0.5 mV s^{-1}. The linear Tafel segments of cathodic and anodic curves were extrapolated to corrosion potential to obtain the corrosion current densities (I_{corr}). The inhibition efficiency ($\eta\%$) were evaluated from the calculated I_{corr} values using the relation [23] :

$$\eta(\%) = \frac{I^o_{corr} - I^i_{corr}}{I^o_{corr}} \times 100 \quad (3)$$

where, I^o_{corr} and I^i_{corr} are the corrosion current densities in absence and presence of various concentrations of the inhibitor, respectively. The linear polarization study was carried out from cathodic potential of – 20 mV vs. OCP to an anodic potential of + 20 mV vs. OCP with a scan rate 0.125 mV s^{-1} to study the polarization resistance (R_p).

EIS measurements were carried out in a frequency range of 100 k Hz to 0.01 Hz with amplitude of 10 mV using ac signals at open circuit potential. The charge transfer resistance values have obtained from the diameter of the semi circles of the Nyquist plots. The inhibition efficiency of the inhibitor was calculated from the charge transfer resistance values using the following equation:

$$\eta\,(\%) = \frac{R_{ct}^{i} - R_{ct}^{o}}{R_{ct}^{i}} \times 100 \qquad (4)$$

where, R_{ct}^{o} and $R_{ct}^{'}$ are the charge transfer resistance in absence and presence of inhibitor, respectively.

3. RESULTS AND DISCUSSION

3.1 Weight loss measurements

3.1.1 Effect of inhibitor concentration

Table 1 shows the values of inhibition efficiencies and corrosion rates obtained from weight loss measurements for different concentrations of CFT in 1.0 M HCl after 3 h immersion at 308 K. It follows that the weight loss decreased (i.e., corrosion rate is suppressed), and therefore the corrosion inhibition strengthened, with increase in inhibitor concentration.

3.1.2 Effect of temperature

The effect of temperature on the performance of the inhibitor at a concentration of 100 ppm for mild steel in 1 M HCl at 308 - 338 K was studied using weight loss measurements as shown in figure 2. The corrosion rate increased with increasing temperature both in free and inhibited acid.

Table 1. Corrosion parameters for mild steel in aqueous solution of 1 M HCl in absence and presence of different concentrations of CFT from weight loss measurements at 308 K for 3h

Name of inhibitor	Conc. Of inhibitor (ppm)	Weight loss (mg cm^{-2})	IE%	CR (mm y^{-1})
CFT	-	10.90	-	4.04
	20	2.95	72.9	1.94
	40	1.24	88.6	0.46
	60	0.82	92.5	0.30
	80	0.53	95.1	0.19
	100	0.51	95.3	0.18

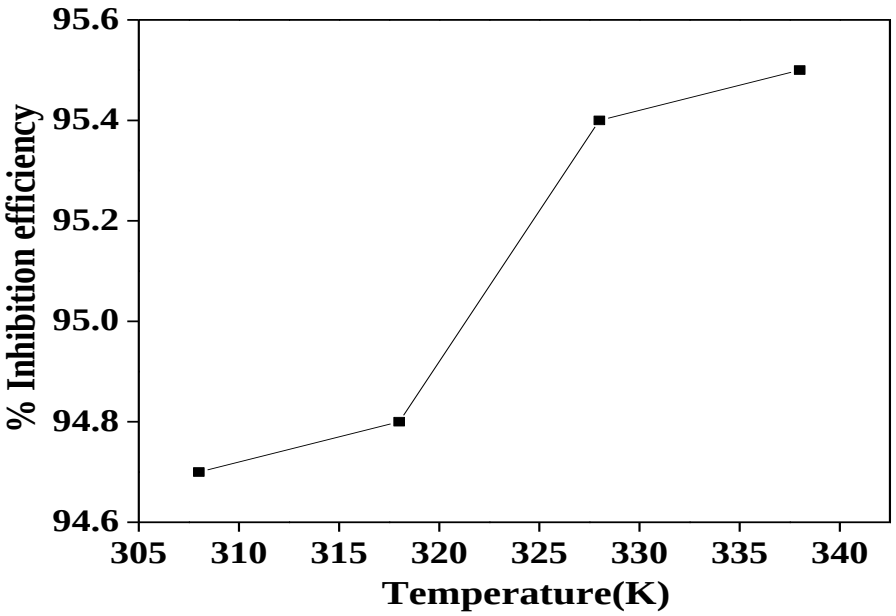

Figure 2. Variation of inhibition efficiency of CFT with temperature

3.2 Adsorption isotherm

Assuming that the corrosion inhibition was caused by the adsorption of these molecules, the degree of surface coverage (θ) for different inhibitor concentrations was evaluated from weight loss measurements as described elsewhere [22].

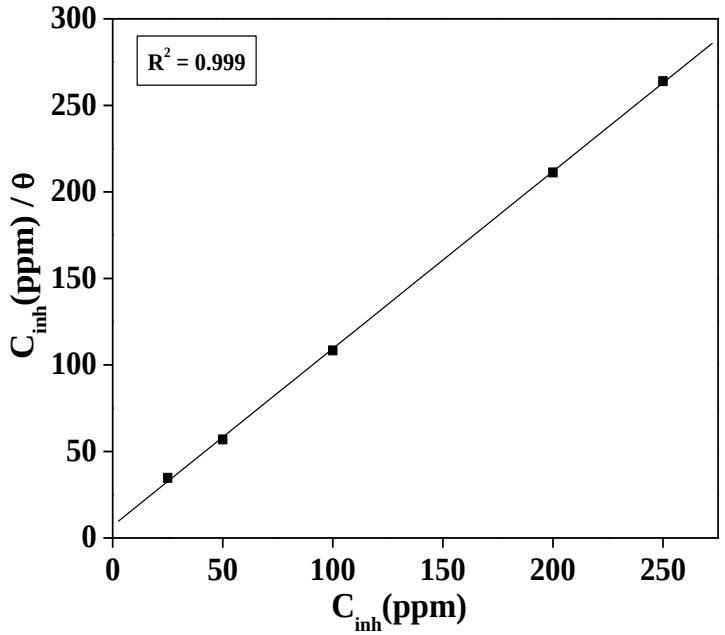

Figure 3. Langmuir adsorption isotherm plot for Cefacetrile (CFT)

The best correlation between the experimental results and isotherm functions was obtained using Langmuir adsorption isotherm. The Langmuir isotherm for monolayer chemisorption is given by the following equation [24]:

$$\frac{C_{inh}}{\theta} = \frac{1}{K} + C_{inh} \quad (5)$$

Where, K is the equilibrium constant of the adsorption process. The plots of C_{inh}/θ vs. C_{inh} gave straight line with nearly unit slope showing that the adsorption of CFT can be fitted to Langmuir adsorption as presented in figure 3.

Adsorption equilibrium constant (K_{ads}) and free energy of adsorption (ΔG^{o}_{ads}) were calculated using the relationships [25]:

$$K_{ads} = \frac{1}{C} \times \frac{\theta}{1-\theta} \quad (6$$

$$\Delta G_{ads} = -2.303RT \log(55.5K_{ads}) \quad (7)$$

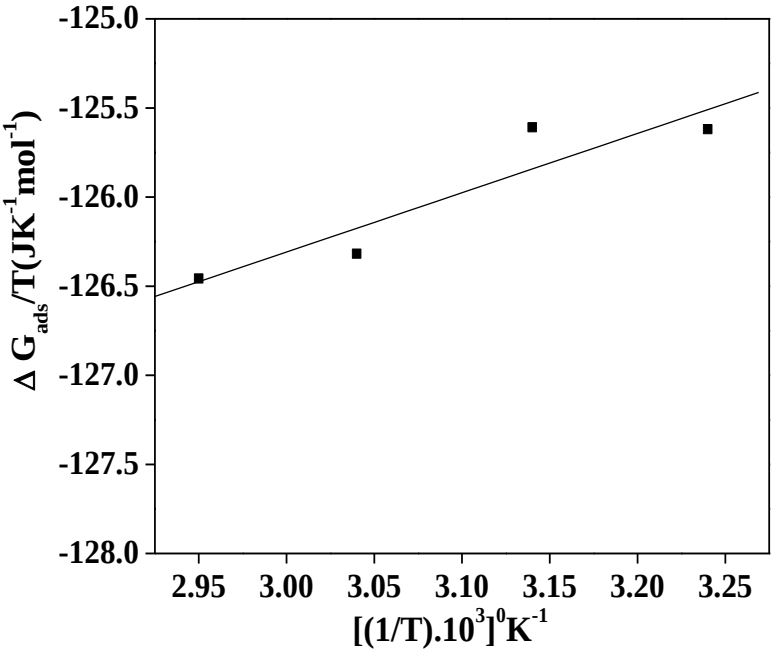

Figure 4. plot of $\Delta G^{o}_{ads}/T$ with $1/T$ Cefacetrile (CFT)

The value of 55.5 is the molar concentration of water in solution [26].

The enthalpy of adsorption was calculated from the Gibbs–Helmholtz equation [27]:

$$\left[\frac{\partial\left(\Delta G^{o}{}_{ads}/T\right)}{\partial T}\right]_{P} = -\frac{\Delta H^{o}_{ads}}{T^{2}} \quad (8)$$

This equation can be arranged to give:

$$\frac{\Delta G^{o}_{ads}}{T} = \frac{\Delta H^{o}_{ads}}{T} + k \quad (9)$$

The plot of $\Delta G^{o}_{ads}/T$ with $1/T$ gives a straight line with slope equal to ΔH^{o}_{ads} (figure 4). It can be seen from the figure that $\Delta G^{o}_{ads}/T$ decreased with $1/T$ in a linear fashion.

According to thermodynamic basic equation (Eq. 10) [28], the entropy of adsorption was calculated.

$$\Delta G^{o}_{ads} = \Delta H^{o}_{ads} - T\Delta S^{o}_{ads} \quad (10)$$

All the obtained thermodynamic parameters are presented in Table 2. The negative sign of ΔH^{o}_{ads} indicated that the adsorption of inhibitor molecules was an exothermic process, and the positive value of ΔS^{o}_{ads} explained in the following way: the adsorption of CFT from the aqueous solution can be regarded as quasi-substitution process between the organic compound in the aqueous phase and water molecules at the mild steel surface [26]. In this situation, the adsorption of CFT is accompanied by desorption of water molecules from the surface.

Thus, as the adsorption of inhibitor is believed to be exothermic and associated with decrease in entropy of the solute, the opposite is true for solvent. Since, the thermodynamic values obtained are the algebraic sum of adsorption of organic inhibitor molecule and desorption of water molecules [29]. Therefore, gain in entropy is attributed to increase in solvent entropy.

The negative values of ΔG^{o}_{ads} indicated that the adsorption of CFT molecule was a spontaneous process. The value of ΔG^{o}_{ads} obtained is – 39.50 kJ mol^{-1} which indicates that the adsorption is not a simple physical adsorption but it may involve some other interactions.

Table 2. Thermodynamic activation parameters for mild steel in 1 M HCl in absence and presence of CFT of 100 ppm concentration

Name of inhibitor	E^{o}_{a} (kJ mol^{-1})	ΔH^{o}_{a} (kJ mol^{-1})	ΔS^{o}_{a} (J mol^{-1} K^{-1})	ΔG^{o}_{ads} (kJ mol^{-1})	ΔH^{o}_{ads} (kJ mol^{-1})	ΔS^{o}_{ads} (J mol^{-1} K^{-1})
1 M HCl	42.72	39.55	-86.75	-	-	-
CF	35.60	32.54	-121.62	-39.50	-8.92	99.29

3.3 Kinetic parameters

The inhibition properties of CFT can be explained by means of kinetic model. The activation parameters were calculated from Arrhenius equation and transition state equation [30, 31]:

To obtain the activation energy, the linear regression between $\log CR$ and $1/T$ was obtained and the relationship between $\log CR$ and $1/T$ is shown in figure 5a. Figure 5b shows the plot of $\log CR/T$ vs. $1/T$. Straight line was obtained with slope of $\left(\Delta H_a^o/2.303R\right)$ and an intercept of $\left[\log\left(R/Nh\right)+\left(\Delta S_a^o/2.303R\right)\right]$, from which the values of ΔSº and ΔHº have been calculated and listed in table 2.

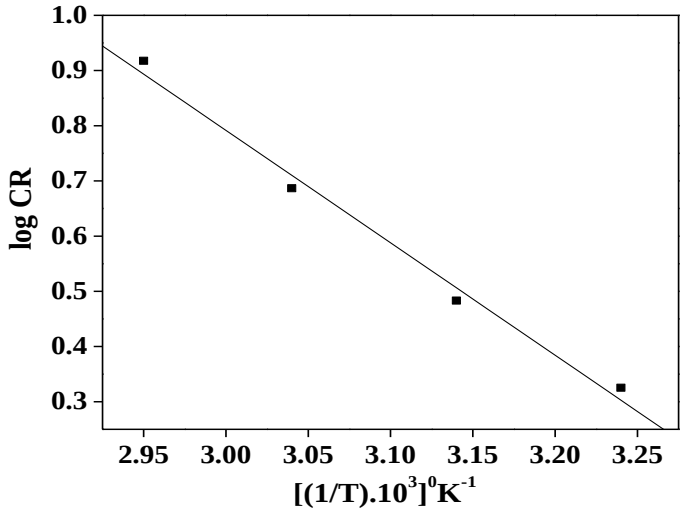

A

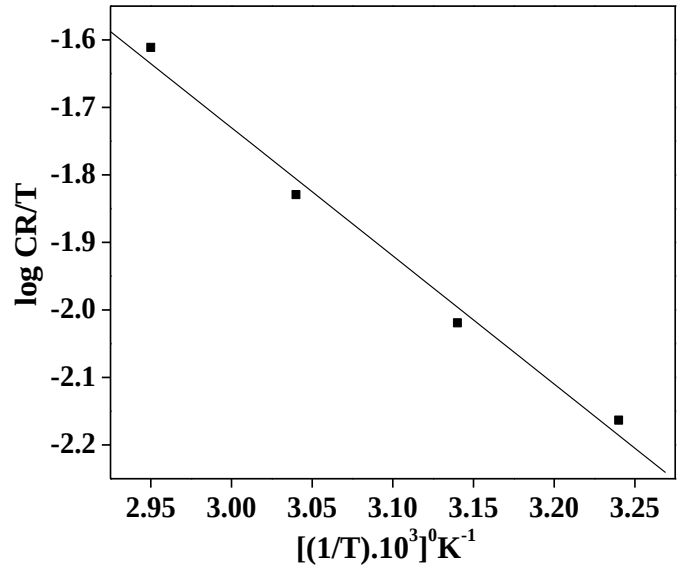

B

Figure 5. (a) Arrhenius plot of log *C*R versus 1/*T* and (b) log (*C*R/*T*) versus 1/*T* at 200 ppm CFT

The positive sign of enthalpy of activation reflected the endothermic nature of dissolution process. From Table 2, it is seen that the value of activation energy and enthalpy of activation varied in the same way. The value of entropy of activation is higher for inhibited solution than that for free acid solution. This suggested that randomness increased on going from reactant to activated complex. This might be due to adsorption of organic adsorbate from the acidic solution could be regarded as quasi-substitution process between the organic compound in the aqueous phase and water molecules at mild steel surface [32]. In this situation, the adsorption of organic inhibitor was accompanied by desorption of water molecules from the surface. Thus the increase in entropy of activation was attributed to the increasing solvent entropy [33].

3.4 Tafel polarization

Tafel polarization curves for mild steel in 1M HCl with and without various concentrations of CFT are shown in figure 6a. Anodic and cathodic current decreased in the presence of inhibitor molecules and this effect increases with the increase in inhibitor concentration. It showed that the addition of inhibitor molecules reduces anodic dissolution of mild steel and also retards the hydrogen evolution reaction. This effect is attributed to the adsorption of inhibitor on the active sites of metal surface [34]. The important corrosion parameters derived from these curves are listed in Table 4. It was found that (Table 3) the values of anodic Tafel slopes were comparatively constant while cathodic Tafel slopes increased; in addition the change in E_{corr} values were in the range of 20 - 25 mV vs. SCE. Thus, CFT is considered as mixed type but predominantly cathodic inhibitor [35].

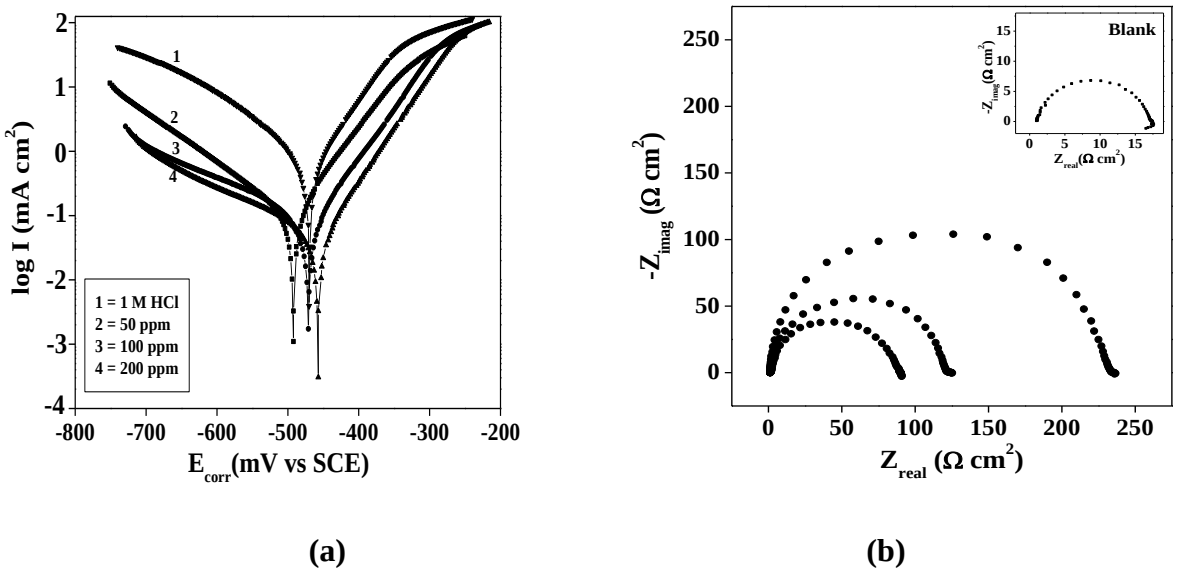

Figure 6. (a) Tafel polarization curves for corrosion of mild steel in 1 M HCl in the absence and presence of different concentrations of CFT (b)) Nyquist plot for the mild steel in 1 M HCl in the absence and presence of CFT.

3.5 Electrochemical impedance spectroscopy

The effect of inhibitor concentration on the impedance behaviour of mild steel in 1M HCl solution at 303 K is presented in figure 6b. The curves show a similar type of Nyquist plot for mild steel in the presence of various concentrations of CFT. The simple equivalent Randle circuit for studies was shown in figure 7, where R_Ω represents the solution and corrosion product film resistance, the parallel combination of resister, R_{ct} and capacitor C_{dl} represents the corroding interface. The existence of single semi circle showed the single charge transfer process during dissolution which is unaffected by the presence of inhibitor molecules. Deviations of perfect circular shape are often refereed to the frequency dispersion of interfacial impedance which arises due to the roughness and other inhomogeneity of the surface [36, 37]. As seen from Table 3, the R_{ct} values of inhibited substrates are increased with the concentration of inhibitors. On the other hand, the values of C_{dl} are decreased with increase in inhibitor concentration which is most probably is due to the decrease in local dielectric constant and / or increase in thickness of the electrical double layer, suggests that CFT act via adsorption at the metal / solution interface [38, 39].

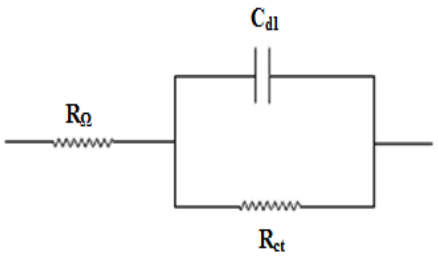

Figure 7. The electrochemical equivalent circuit used to fit the impedance measurements

Table 3. Electrochemical parameters for corrosion of mild steel in 1M HCl in the presence of different concentrations CFT.

	Tafel data					Impedance data		
Conc. Of Inhibitor (ppm)	E_{corr} (mV vs SCE)	I_{corr} (μA cm^{-2})	β_a (mV / dec)	β_c (mV / dec)	IE%	R_{ct} (Ω cm^2)	C_{dl} (μFcm^{-2})	IE
0	-469	730	73	127	-	17.3	1006	-
40	-489	112	70	135	85.4	145.2	136	88.1
60	-470	86.1	71	200	88.6	192.0	79	90.9
100	-460	49.7	65	193	93.7	371.2	73	95.3

4. MECHANISM OF INHIBITION

Corrosion inhibition of mild steel in 1 M HCl by CFT can be explained on the basis of molecular adsorption. The studied compound inhibits corrosion by controlling both the anodic and

cathodic reactions. Cefacetrile is an organic compound containing heteroatom, upon addition of an acid to the aqueous solution of this compound will transform the neutral molecule to the cation. Inhibitor molecules could be adsorbed on the metal surface by sharing of electrons in the form of neutral molecules. The performance of CFT in acid media can be explained in the following way. In aqueous acid solutions, the CFT exists either as neutral molecule or in the form of cation.

The process of the adsorption is influenced by the nature and the charge of the metal, by the chemical structure of the organic inhibitor and the type of aggressive electrolyte. The charge of the metal surface can determined from the potential of zero charge (pzc) on the correlative scale (Ψ_c) [40] by the equation:

$$\psi_c = E_{corr} - E_{q=0} \quad (13)$$

where, $E_{q=0}$ is the potential of zero charge. However, value of E_{corr} obtained in HCl solution ranged from – 469 to – 460 mV vs. SCE. Benerijee and Malhotra [41] reported the pzc of iron in HCl solution is - 530 mV vs. SCE, therefore, the metal surface becomes slightly positively charged. Hence, Cl^- ions are adsorbed on the metal surface. Due to electrostatic attraction, protonated CFT are physically adsorbed and high inhibition efficiency is expected [42]. Upon the formation, ion pairs and molecules reorient so that inhibitor molecules becomes parallel to the mild steel surface. This orientation leads to interaction of unshared pairs of electrons of N atoms and π-electrons of aromatic ring and vacant d-orbitals of surface iron atoms. Thus, the protonated species adsorbed on the cathodic sites of the mild steel and decrease the evolution of hydrogen. CFT adsorbed on anodic sites through lone pair of electrons of nitrogen atom and π-electrons of aromatic ring and hence, anodic dissolution of mild steel is decreased.

5. CONCLUSIONS

1. The inhibition efficiency of CFT increases with increase in inhibitor concentration.
2. The inhibitor showed maximum inhibition efficiency 94.7% at 100 ppm concentration.
3. Langmuir adsorption isotherm and impedance studies showed that CFT inhibits through adsorption mechanism.
4. Potentiodynamic polarization reveals that CFT acted as mixed-type predominantly cathodic inhibitor.

ACKNOWLEDGEMENT
AKS and SKS are thankful to North-West University, Republic of South Africa for Post Doctoral Fellowship.

References

1. A.S. Fouda, H.A. Mostafa, F. El-Taib Haekel, G.Y. Elewady, *Corros. Sci.* 47 (2005) 1988.

2. P.C. Okafor, Y. Zheng , *Corros. Sci.* 51 (2009) 850.
3. H.L. Wang, R.B. Liu, J. Xin, *Corros. Sci.* 46 (2004) 2455.
4. G.E. Badr, *Corros. Sci.* (2009), doi: 10.1016/j.corsci.2009.06.017
5. M.S. Morad , A.A.O. Sarhan, *Corros. Sci.* 50 (2008) 744.
6. M.G. Hosseini, M. Ehteshamzadeh, T. Shahrabi, *Electrochimica. Acta* 52 (2007) 3680.
7. E. Machnikova, K.H. Whitmire, N. Hackerman, *Electrochimica. Acta* 53 (2008) 6024.
8. M.A. Quraishi, I. Ahamad, A.K. Singh, S.K. Shukla, B. Lal, V. Singh, *Mater. Chem. Phys*. 112 (2008) 1035.
9. G. Gunasekaran, L.R. Chauhan, *Electrochimica. Acta* 49 (2004) 4387.
10. S. Varvara, L.M. Muresan, K. Rahmouni, H. Takenouti, *Corros. Sci.* 50 (2008) 2596.
11. G. Singh, L. Jha, R. Mohapatra, *J. Electrochem. Soc. (India)* 39 (1) (1990) 44.
12. S. K. Shukla, M. A. Quraishi, *J. Appl. Electrochem.* DOI 10.1007/s10800-009-9834-1
13. G. Moretti, F. Guidi, G. Grion, *Corros. Sci.* 46 (2004) 387.
14. F.C. Giacomelli, C. Giacomelli, M.F. Amadori, V. Schmidt, A. Spinelli, *Mater. Chem. Phys.* 83 (2004) 124.
15. E.S. Ferreira, C. Giacomelli, F.C. Giacomelli, A. Spinelli, *Mater. Chem. Phys.* 83 (2004) 129.
16. E.E.F. El Sherbini, *Mater. Chem. Phys.* 61 (1999) 223.
17. A.K. Singh, M.A. Quraishi, *Corros. Sci.* 52 (2010) 1529.
18. A.K. Singh, M.A. Quraishi, *Corros. Sci.* 53 (2011) 1228.
19. M. S. Morad, *Corros. Sci*. 50 (2008) 436.
20. M. Abdallah, *Corros. Sci.* 46 (2004) 1981.
21. S.K. Shukla, M.A. Quraishi, R. Prakash, *Corros. Sci.* 50 (2008) 2867.
22. K.F. Khaled, M.A. Amin, *Corros. Sci.* (2009), doi:10.1016/j.corsci.2009.05.023
23. M. Behpour, S.M. Ghoreishi, N. Soltani, M. Salavati-Niasari, M. Hamadanian, A. Gandomi, *Corros. Sci.* 50 (2008) 2172.
24. A.Y. Musa, A.A.H. Kadhum, A.B. Mohamad, A.R. Daud, M.S.Takriff, S.K. Kamarudin, *Corros. Sci.* (2009), doi:10.1016/j.corsci.2009.06.024
25. M.S. Morad, A.M. Kamal El-Dean, *Corros. Sci.* 48 (2006) 3398.
26. L. Tang, G. MU, G. Liu, *Corros. Sci.* 45 (2003) 2251.
27. M.A. Amin, S.S. Abd El Rehim, H.T.M. Abdel-Fatah, *Corros. Sci.* 51 (2009) 882.
28. H. Ashassi-Sorkhabi, B. Shaabani, D. Seifzadeh, *Appl. Surf. Sci.* 239 (2005) 154.
29. V. Branzoi, F. Branzoi, M. Baibarac, *Mater. Chem. Phys.* 65 (2000) 288.
30. A.Ostovari, S.M. Hoseinieh, M. Peikari, S.R. Shadizadeh, S.J. Hashemi *Corros. Sci.* (2009), doi:10.1016/j.corsci.2009.05.024
31. L. del Campo, R.B. Pérez-Sáez, L. González-Fernández, M.J. Tello, *Corros. Sci.* 51 (2009) 707.
32. X. Li, S. Deng, H. Fu, G. Mu, *Corros. Sci.* 51 (2009) 620.
33. B. Ateya, B.E.El-Anadouli, F.M.El-Nizamy, *Corros. Sci.* 24 (1984) 509.
34. M.A. Quraishi, S. Ahmad, G. Venkatachari, *Bull Electrochem* 12 (1996) 109.
35. H. Derya Lec_e, Kaan C. Emregul , Orhan Atakol, *Corros. Sci.* 50 (2008) 1460.
36. J. Aljourani, K. Raeissi, M.A. Golozar, *Corros. Sci.* (2009), doi:10.1016/j.corsci.2009.05.011
37. O. Benali, L. Larabi, M. Traisnel, L. Gengembra, Y. Harek, *Appl. Surf. Sci.* 253 (2007) 6130.
38. M.A. Quraishi, J. Rawat, *Mater. Chem. Phys.* 70 (2001) 95.
39. M.A. Amin, S.S.A. El-Rehim, E.E.F. El-Sherbini, R.S. Bayoumy, *Electrochimica. Acta* 52 (2007) 3588.
40. A.Hermas, M.S. Morad, M.H. Wahdan, *J. Appl. Electrochem.* 34 (2004) 9.
41. G. Benerijee, S.N. Malhotra, *Corrosion (NACE)* 48 (1992) 10.
42. A.K. Singh, M.A. Quraishi, *Corros. Sci.* (2009), doi: 10.1016/j.corsci.2009.07.011